International Journal on Emerging Technologies **10**(2b): 119-125(2019)

ISSN No. (Print) : 0975-8364
ISSN No. (Online): 2249-3255

Mhd Nanofluid Flow Over Stretching/Shrinking Surface in Presence of Heat Radiation Using Numerical Method

B. Mohanty[1], S. Jena[1] and P.K. P attnaik[2]

[1]Department of Mathematics, Centurion University of Technology and Management, Odisha, India.
[2]Faculty, Department of Mathematics, College of Engineering and Technology, Bhubaneswar, Odisha, India.

(Corresponding author : S. Jena)
(Received 02 May 2019, Revised 10 July 2019, Accepted 08 August 2019)
(Published by Research Trend, Website: www.researchtrend.net)

ABSTRACT: This paper considered for an unsteady 2-D stagnation point flow over stretching/shrinking surface. Here the comparison of two nanofluids (Copper Oxide CuO and Aluminum Oxide Al_2O_3) are taken into account by considering the important nano energy conversion parameters. Using similarity variable and stream function the governing PDE's along with continuity, momentum, energy and concentration are converted to respective ODE's and solved using numerical method (Runge-Kutta 4th order). The novelty of all the physical parameters along with Nusselt number and Sherwood number has been discussed by graphical method.

Keywords: Nanofluid, stretching/shrinking surface, Runge-Kutta.

Nomenclature

C_f	Wall skin friction coefficient
C_W	Wall surface concentration f Dimensionless stream function
B_{20}	Strength of magnetic field
L_e	Lewis number
M	Magnetic parameter
Nu	Local Nusselt number
q_r	radiative heat flux
k	Thermal conductivity
Re_x	Local Reynolds number
Sh	Sherwood number
T_w	Constant temperature at the sheet
T_∞	Ambient fluid temperature
K_{nf}	Thermal conductivity
A	Unsteadiness parameter U_w Stretching velocity of the sheet
N_r	Radiation parameter
P_r	Prandtl number
η	Similarity variable
ε	Streching/shrinking parameter
θ	Dimensionless temperature
ψ	Stream function
σ	Electrical conductivity of the fluid
ξ_{nf}	Dimensionless constant
ν_{nf}	Kinematic fluid viscosity
ρ_{nf}	Nanofluid density
μ_{nf}	Dynamic viscosity of nanofluid
α_{nf}	Thermal diffusivity

I. INTRODUCTION

Due to huge number of useful applications in industry and modern engineering technology nanotechnology brought multidimensional uses. Nanofluids consist of nano particles along with base fluids which increases the heat transfer capacity of coolant and it is very highly used in quick heat transfer. Nagaranjan *et al.*, [1] have recently focused the amount of nanoparticle in base fluid and its use in solar collector. In 1995 Choi [2] has given a concept of nanofluid which contains the nanoparticle size whose diameter is less than 50 nm. The boundary layer nanofluid flow concept was then developed by Khan *et al.*, [3]. Then after Makinde *et al.,* [4] analysed the effects of flow of nanofluid in a stretching surface.

Dutta *et al.*, [5] discussed the combined effect of temperature distribution on a stretching sheet along with temperature when a uniform heat flux is added. Mahapatra *et al.,* [6] have examined the combined effect of stagnation point flow and stretching surface effects. Alinia *et al.,* [7] and Bararnia *et al.,* [8] have examined different fluids such as viscoelastic and micro-polar on stretching sheets because of popularity and applications of flow through stretching surface. Analysis of heat and mass transfer with MHD and chemical reaction effects on viscoelastic fluid over a stretching sheet has been discussed by Mishra *et al.,* [9]. Recently Pattnaik *et al.,* [10] have analysed effect of slip boundary conditions on MHD nanofluid flow. Chemical reaction effect on MHD viscoelastic fluid flow over a vertical stretching sheet with heat source/sink has been investigated by *et al.,* [11].

Rout *et al.,* [12] have employed Runge-Kutta fourth order method along with shooting technique to analyse chemical reaction effect on MHD free convection flow in a micropolar fluid. Mishra and Jena [13] investigated the numerical solution of boundary layer MHD flow with viscous dissipation. Recently, Tripathy *et al.*, [14] have investigated the chemical reaction effect on MHD free convective surface over a moving vertical plane through porous medium. Pattnaik and Biswal [15, 16] studied the analytical behaviour of the solution of MHD flow in presence of porosity parameter.

Nanofluid is prepared when nanometersized particles are suspended in basic fluids like Convectional heat transfer fluids. The thermal conductivity plays an important role for heat transfer between heat transfer surfaces and medium both so there are vast methods used to maintain the thermal conductivity by introducing the nano particle in liquids. Many researchers [17-21] have employed numerical techniques on modeling of nanofluids.

The aim of the present paper is to discuss the analytic numerical for unsteady MHD flow past a stretching surface and a comparison between two nanofluids

Copper Oxide (CuO) and Aluminum Oxide (Al_2O_3). The method employed for the numerical solution of nonlinear problem is Runge-Kutta fourth order method.

II. MATHEMATICAL ANALYSIS

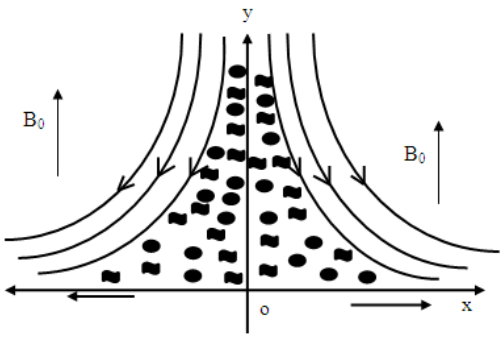

Fig. 1. Flow geometry.

Let consider a 2-D unsteady boundary layer nanofluid flow over a stretching/shrinking sheet with considering thermal radiation. X-axis is measured as distance along the sheet and Y-axis is distance normal to the sheet as well as to the fluid. The fluid flow is confined to $y > 0$. Two equal and opposite forces are applied along x-axis to initiate the formation of the fluid. The fluid flow is steady when $t < 0$ and when $t = 0$ the fluid is unsteady. The governing continuity, momentum, energy and concentration equations of such type of flow is written as

$$\frac{\partial u}{\partial x}+\frac{\partial v}{\partial y}=0 \tag{1}$$

$$\frac{\partial u}{\partial t}+u\frac{\partial u}{\partial x}+v\frac{\partial v}{\partial y}=\nu_{nf}\frac{\partial^2 u}{\partial y^2}-\frac{\sigma B_0^2 u}{\rho_{nf}} \tag{2}$$

$$\frac{\partial T}{\partial t}+u\frac{\partial T}{\partial x}+v\frac{\partial T}{\partial y}=\alpha_{nf}\frac{\partial^2 T}{\partial y^2}-\frac{1}{(\rho C_p)_{nf}}\frac{\partial q_r}{\partial y} \tag{3}$$

$$\frac{\partial C}{\partial t}+u\frac{\partial C}{\partial x}+v\frac{\partial C}{\partial y}=D_B\frac{\partial^2 C}{\partial y^2}-\gamma_0(C-C_\infty) \tag{4}$$

The appropriate boundary conditions are

$$\left.\begin{aligned} &u=U_w(x,t), v=0, T=T_w(x,t), C=C_w(x,t) && \text{at } y=0,\\ &u\to U(x), T\to T_\infty, C\to C_\infty && \text{as } y\to\infty \end{aligned}\right\} \tag{5}$$

$$\left.\begin{aligned} &\mu_{nf}=\frac{\mu_f}{(1-\phi)^{2.5}}, \alpha_{nf}=\frac{k_{nf}}{(\rho c_p)_{nf}}, k_{nf}=k_f\frac{(k_s+2k_f)-2\phi(k_s-k_f)}{(k_s+2k_f)+\phi(k_s-k_f)}\\ &(\rho Cp)_{nf}=(\rho Cp)_f(1-\phi)+(\rho Cp)_s\phi, q_r=-\frac{4\sigma\partial T^4}{3k_1\partial y} \end{aligned}\right\} \tag{6}$$

III. TRANSFORMATION OF GOVERNING EQUATIONS

The stretching velocity is considered as $U_w(x,t)=\frac{ax}{1-\alpha t}$ where a and a are constants, the temperature of the sheet is $T_w=T_\infty+\frac{bx}{(1-\alpha t)^2}$ and the wall surface concentration is $C_w=C_\infty+\frac{bx}{(1-\alpha t)^2}$.

The continuity Eqn. (1) satisfies by introducing similarity function ψ such that $u=\frac{\partial\psi}{\partial y}, v=-\frac{\partial\psi}{\partial x}$

To discuss the existence of similarity let us assume

$$\left.\begin{aligned} &\eta=\left(\sqrt{a/\nu}\Big/\sqrt{1-\alpha t}\right)y,\ u=\left(ax/1-\alpha t\right)f'(\eta),\\ &v=-\left(\sqrt{a\nu/1-\alpha t}\right)f(\eta), \theta(\eta)=\frac{T-T_\infty}{T_w-T_\infty},\\ &\Phi(\eta)=\frac{C-C_\infty}{C_w-C_\infty}, q_r=-\frac{4\sigma}{3k_1}\frac{\partial T^4}{\partial y},\\ &\psi(x,y)=\left(\sqrt{a\nu/1-\alpha t}\right)xf(\eta) \end{aligned}\right\} \tag{7}$$

Using Eqn. (7) the governing Eqns. (2-4) are converted in to following ODE's as follows

$$\frac{1}{(1-\phi)^{2.5}\left(1-\phi+\phi\frac{\rho_s}{\rho_f}\right)}f'''-f'^2 + ff''-Mf'-A\left(f'+\frac{\eta}{2}f''\right)=0 \tag{8}$$

$$\frac{1}{\frac{k_f}{k_{nf}}\left(1-\phi+\phi\frac{(\rho C_p)_s}{(\rho C_p)_f}\right)}\theta'' +\frac{P_r}{(1+N_r)}\left\{f\theta'-f'\theta-A\left(2\theta+\frac{\eta}{2}\theta'\right)\right\}=0 \tag{9}$$

$$\Phi''+L_eP_r\left\{\begin{aligned}&(f'\Phi-f\Phi')\\ &-A\left(2\Phi+\frac{\eta}{2}\Phi'\right)-\xi\Phi\end{aligned}\right\}=0 \tag{10}$$

With boundary conditions

$$\left.\begin{aligned} &f'(0)=\varepsilon,\ \theta(0)=1, \Phi(0)=1 && \text{at } \eta=0,\\ &f'(\eta)\to 0, \theta(\eta)\to 0, \Phi(0)\to 0 && \text{as } \eta\to\infty, \end{aligned}\right\} \tag{11}$$

IV. SKIN FRICTION, HEATTRANSFERANDMASS TRANSFERCOEFFICIENT

Skin friction coefficient $C_f=\frac{\mu}{\rho_f U_w^2}\left(\frac{\partial u}{\partial y}\right)_{y=0}$

The non-dimensional form is $C_f\sqrt{\mathrm{Re}_x}=f''(0)$

Local Nusselt number $Nu_x=\frac{x}{k(T_w-T_\infty)}\left(k\left(\frac{\partial T}{\partial y}\right)_{y=0}-\frac{4\sigma}{3k_1}\left(\frac{\partial T^4}{\partial y}\right)_{y=0}\right)$

The non-dimensional form is $Nu_x\sqrt{\mathrm{Re}_x}=-(1+N_r)\theta'(0)$

Sherwood number $Sh_x=-\frac{x}{k(T_w-T_\infty)}\left(\frac{\partial C}{\partial y}\right)_{y=0}$

The non-dimensional form is $Sh_x\sqrt{\mathrm{Re}_x}=-\Phi'(0)$

V. NUMERICAL RESULTSAND DISCUSSIONS

The Eqns. (8)-(10) are solved by implementing numerical technique using the fourth order Runge-Kutta method on a computer program which is written in Matlab software. A suitable step size was adopted for the result. The values for the velocity, temperature and concentration profiles and also the skin-friction coefficients, Nusselt numbers and Sherwood numbers have been obtained for various parametric conditions and presented in graphical form. The summarized results are given in following paragraphs.

Fig. 2 shows the variation of velocity with different nanoparticle volume fractions for both CUO and (Al_2O_3).

Here the comparison also occurs against stretching $(\varepsilon = 1)$ and shrinking $(\varepsilon = -1)$ parameters both the cases. This has been observed that for $\varepsilon = 1$ the velocity profile increases as nanoparticle volume fraction increases for both CUO and (Al_2O_3). But it has been noticed that CUO as compared to Al_2O_3 has largest velocity. Again exactly the reverse results has been encountered for the reverse case $(\varepsilon = -1)$.

From Fig.3 it has been observed that magnetic parameter (M) decreases the velocity profile significantly for stretching case and also Al_2O_3 carries maximum velocity as compared with CUO. On the other hand shrinking parameter $(\varepsilon = -1)$ carries exactly the reverse case. But nearly about η = 6 a stagnation point characteristic occurs.

Fig. 4 reveals the variation of on steadiness parameter (A). This has been observed that for $\varepsilon = 1$, A increases the velocity profile irrespective of CUO and Al_2O_3. An Interesting results has been encountered in case of $\varepsilon = -1$ that, an increases the velocity profile up to $\eta = 1.5$ but after η = 1.5 the velocity profile decreases significantly.

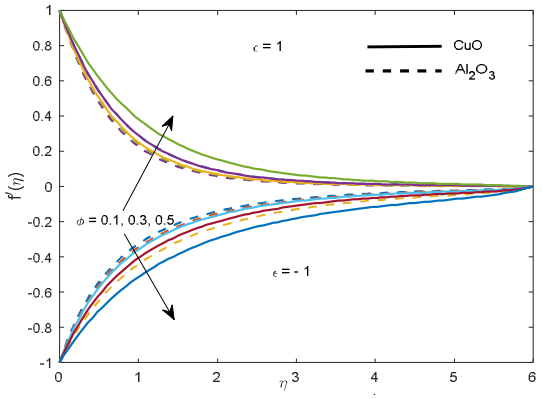

Fig. 2. Variation of Velocity Profile f' (η) with ϕ.

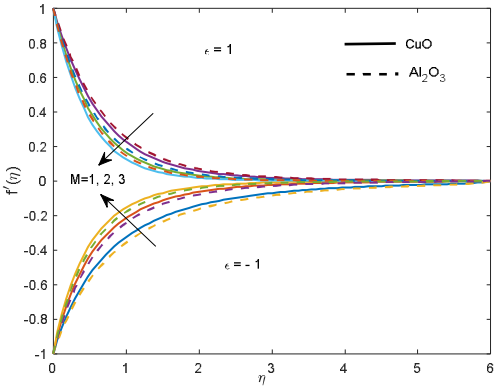

Fig. 3. Variation of Velocity Profile f' (η) with M.

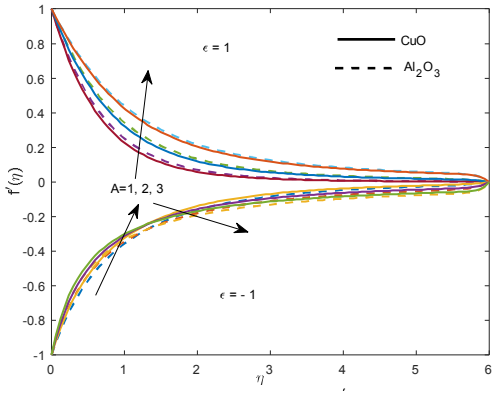

Fig. 4. Variation of Velocity Profile f' (η) with A.

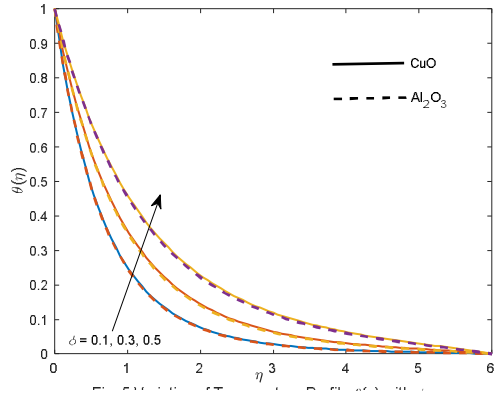

Fig. 5. Variation of Temperature Profile $\theta(\eta)$ with ϕ.

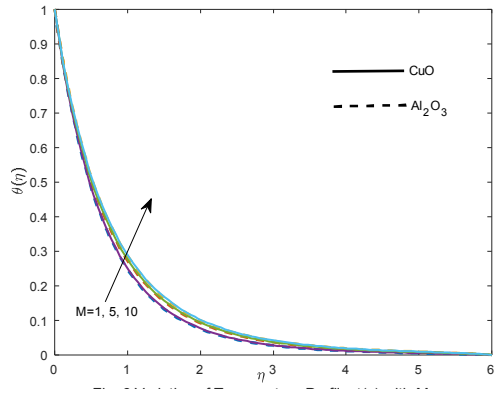

Fig. 6. Variation of Temperature Profile $\theta(\eta)$ with M.

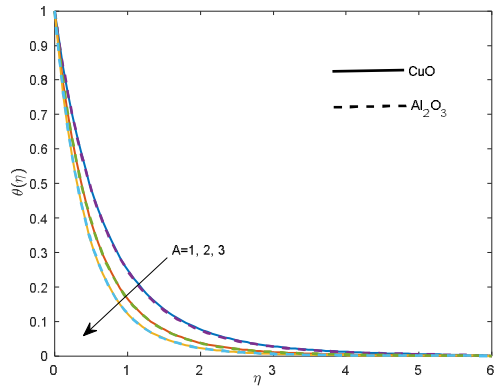

Fig. 7. Variation of Temperature Profile $\theta(\eta)$ with A.

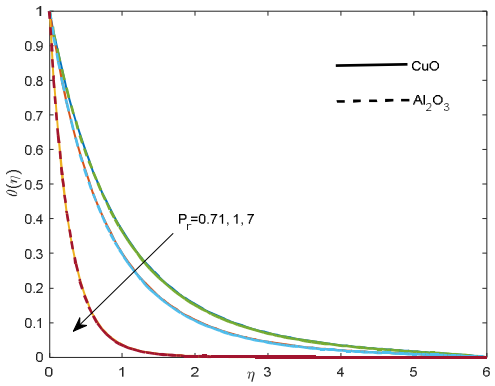

Fig. 8. Variation of Temperature Profile θ(η) with P_r.

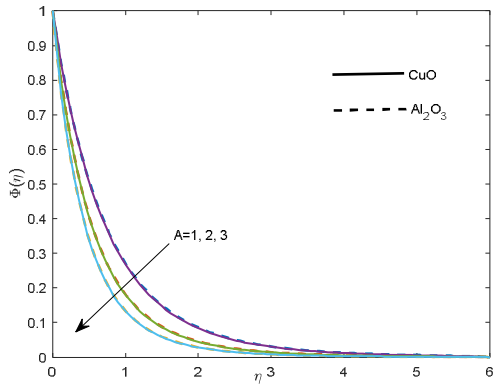

Fig. 12. Variation of Concentration Profile Φ(η) with A.

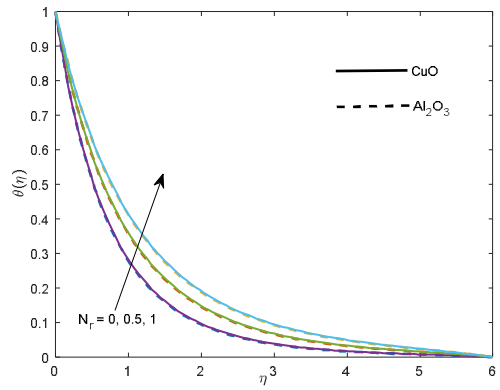

Fig. 9. Variation of Temperature Profile θ(η) with N_r.

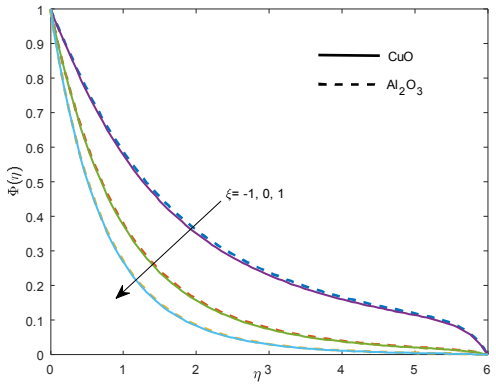

Fig. 13. Variation of Concentration Profile Φ(η) with ξ.

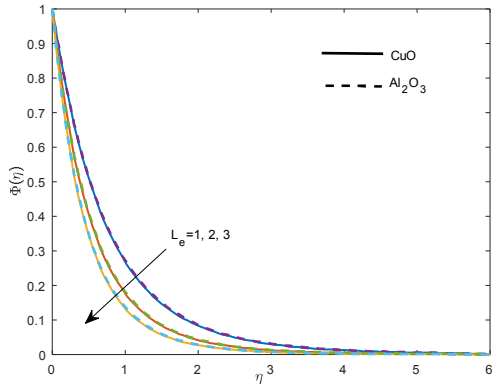

Fig. 10. Variation of Concentration Profile Φ(η) with L_e.

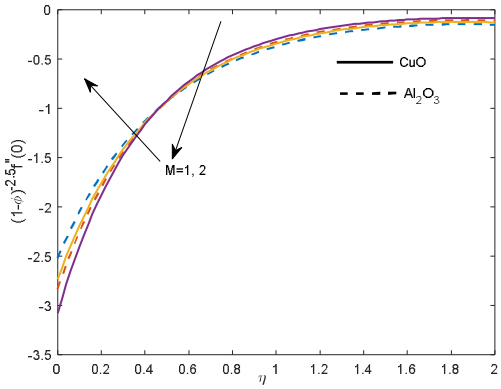

Fig. 14. Variation of Skin friction coefficient with M.

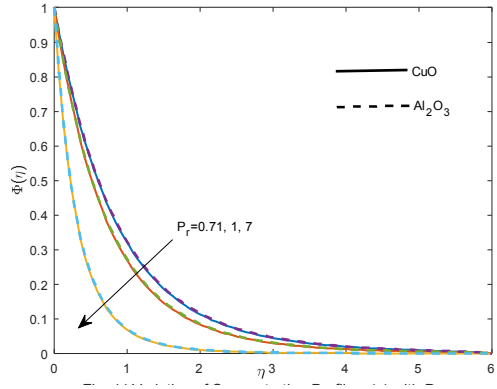

Fig. 11. Variation of Concentration Profile Φ(η) with P_r.

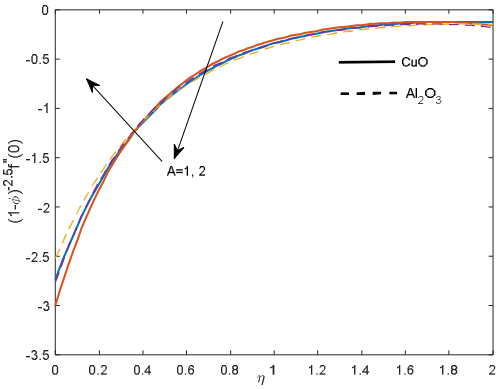

Fig. 15. Variation of Skin friction coefficient with A.

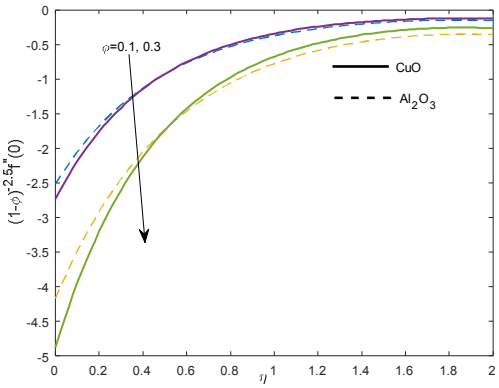

Fig. 16. Variation of Skin friction coefficient with ϕ.

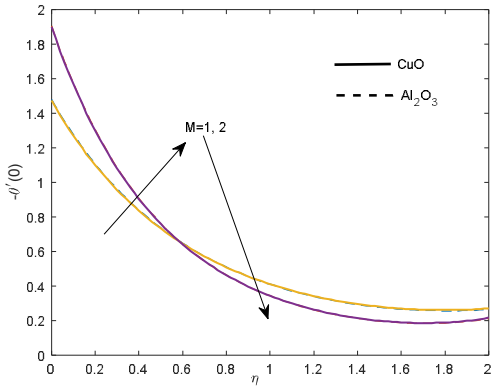

Fig. 17. Variation of Nusselt Number with M.

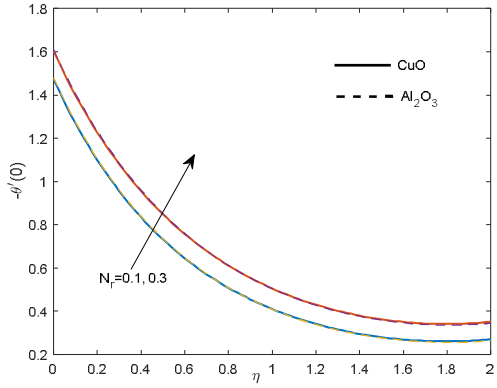

Fig. 18. Variation of Nusselt Number with N_r.

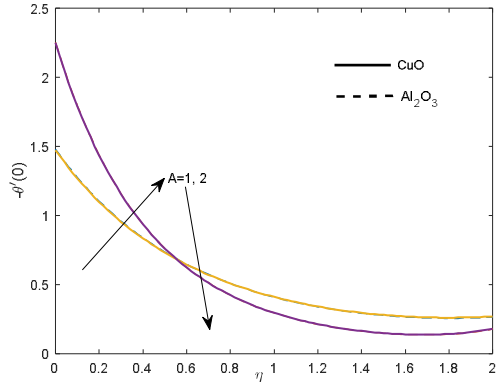

Fig. 19. Variation of Nusselt Number with A.

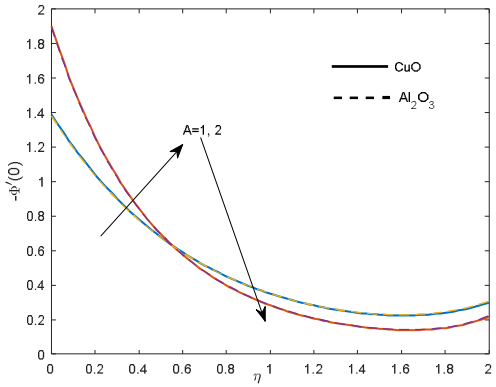

Fig. 20. Variation of Sherwood Number with A.

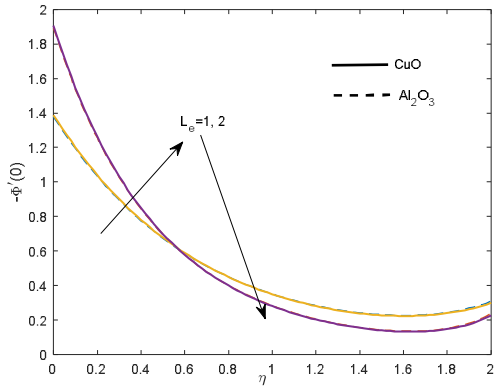

Fig. 21. Variation of Sherwood Number with L_e.

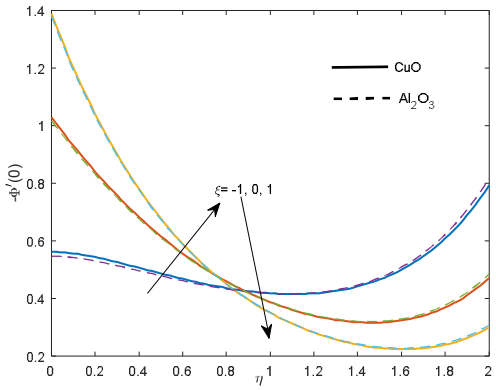

Fig. 22. Variation of Nusselt Number with ξ.

From Fig. 5 it is remarked that, ϕ increases the temperature profile in both CUO and Al_2O_3 cases but there is slight difference between CUO and Al_2O_3 for the same value of ϕ. However the CUO possesses a little high temperature then Al_2O_3.

Fig. 6 exhibit the effect of the magnetic parameter on temperature profile. It is evident that the magnetic field increases the temperature at all the layers and CUO possesses maximum temperature then Al_2O_3. Figs. 7, 8 depict variation of temperature profile with A and P_r respectively. It is observed that, A & P_r decreases the temperature at all the layers. Fig. 9 shows the effects of N_r on temperature profile. Temperature profile increases with increasing value of N_r and also there is a negligible difference between CUO and Al_2O. However CUO of obtains maximum temperature then Al_2O_3.

Figs. 10, 11, 12 and 13 shows the variation of concentration profile with respect to L_e, P_r , A and ξ for

both CUO and Al_2O_3 cases. In each case it has been noticed that all the above respective parameters decreases the concentration profile with increasing value of parameters. Another result in each figure has been noticed that Al_2O_3 increases the concentration profile then CUO.

Figs. 14, 15 graphically shows the skin friction coefficient with M and A. An interesting result in both the cases has been taken into account that nearly about $\eta = 0.5$ the increasing rate of screen with respect to M and A meets. Again after $\eta = 0.5$ the variation shows the reverse effect for both CUO / Al_2O_3. Fig. 16 gives the skin variation with ϕ. We observed that 'ϕ' decreases the profile irrespective of Al_2O_3 / CUO. Again after η = 0.5 the reverse effect is noticed.

Fig. 17 gives the variation of Nusselt number with 'M'. M increases the profile up to η = 0.5 then after decreases for both CUO and Al_2O_3 and a negligible effect reveals for CUO and Al_2O_3.

Fig. 18 is for Nusselt Number with respect N_r. The radiation parameter increases Nusselt number for both CUO and Al_2O_3. Fig. 19 gives the same result as figure 17 so as 'A' has the same effect like 'M'.

Figs. 20, 21 displays variation of Sherwood number with 'A' and 'L_e' respectively. In both cases the profile increases up to $\eta = 0.5$ then after decreases for both CUO & Al_2O_3.

Fig. 22 gives an interesting result for Nusselt number with 'ξ'. The profile increases up to $\eta = 0.7$ then after decreases.

VI. CONCLUSION

- Velocity in stretching case $(\varepsilon = 1)$ and temperature profiles increases as nanoparticle volume fraction increases for both CUO and Al_2O_3.

- Magnetic parameter (M) decreases the velocity profile for stretching case $(\varepsilon = 1)$ but increases shrinking case $(\varepsilon = -1)$ where as temperature increases in same case.

- P_r decreases both temperature and concentration profiles whereas N_r increases the temperature.

- ϕ decreases the skin friction and N_r increases the Nusselt number.

ACKNOWLEDGEMENT

This study was supported by Centurion University of Technology and management through support of all Authors and Mathematics department of Centurion University.

CONFLICT OF INTEREST

Authors have no any conflict of interest.

REFERENCES

[1]. Nagarajan, P. K., Subramani, J., Suyambazhahan, S., & Sathyamurthy, R. (2014). Nanofluids for solar collector applications a review. *Energy Procedia*, 61: 2416–34,

[2]. Choi, S. U. S., Eastman, J. A. (1995). Enhancing thermal conductivity of fluids with nanoparticles. USA, ASME, FED 231/MD 66: 99.

[3]. Khan, W.A., & Pop, I., (2010). Boundary-layer flow of a nanofluid past a stretching sheet. *Int. J. Heat Mass Tran*. 53: 2477.

[4]. Makinde, O. D., & Aziz, A., (2011). Boundary layer flow of a nanofluid past a stretching sheet with a convective boundary condition. *Int. J. Therm.Sci.* 50:1326.

[5]. Nallapu, Dutta, B. K., Roy, P., & Gupta, A.S. Temperature field in flow over a streatching sheet with uniform heat flux, *Int. Comm. Heat Mass Transfer*,12: 89.

[6].Mahapatra, T. R., & Gupta, A. S., (2003), Stagnation-point flow flow towards a stretching surface. *Can. J. Chem. Eng*, 81: 258-263.

[7]. Alinia, M., Domairry, G., Gorji, M., Zahedi, A., & Soleimani, S., (2011), Analysis on viscoelastic fluid flow and heat transfer over a stretching sheet. *Int. J. Comput. Methods Eng. Sci. Mech*, 12:78-289.

[8]. Baramia, H., Ghasemi, E., Domairry, G., & Soleimani, S., (2010). Behavior of micro-polar flow due to linear stretching of porous sheet with injection and suction, Adv. Eng. Softw, 41:893-897.

[9]. Mishra, S. R., Pattnaik, P. K., Bhatti, M.M., & Abbas, T. Analysis of heat and mass transfer with MHD and chemical reaction effects on viscoelastic fluid over a stretching sheet. *Indian J Phys*, DOI 10.1007/s12648-017-1022-2.

[10]. Pattnaik, P. K., Mishra, N., & Muduly, M. M..(October 2018) effect of slip boundary conditions on MHD nanofluid flow, EPRA International Journal, Vol: 3, Issue: 10

[11]. Jena, S., Dash, G. C., & Mishra, S.R. (2018), Chemical reaction effect on MHD viscoelastic fluid flow over a vertical stretching sheet with heat source/sink, Ain Shams Eng. J., 9:1205-1213.

[12]. Rout, P. K., Sahoo, S. N., Dash, G. C., & Mishra, S. R., (2016). Chemical reaction effect on MHD free convection flow in a micropolar fluid, Alexandria Eng. J., 55 no. 3:2967-2973

[13]. Mishra, S. R., Jena, S., (2014). Numerical solution of boundary layer MHD flow with viscous dissipation. *The Scientific World Journal*. Article ID 756498, 5 pages.

[14]. Tripathy, R. S., Dash, G. C., Mishra, S. R., & Baag, S. (2015). Chemical reaction effect on MHD free convective surface over a moving verticle plane through popous medium. *Alexandria Engineering Journal*, 54(3):673-679

[15]. Pattnaik, P. K., & Biswal, T., (2015). Analytical Solution of MHD Free Convective Flow through Porous Media with Time Dependent Temperature and Concentration, *Walailak J Sci. & Tech*. **12** (9) : 749-762

[16]. Pattnaik, P. K., & Biswal, T. (2015). MHD free convective boundary layer flow of a viscous fluid at a vertical surface through porous media with non-uniform heat source, *IJISET*, **2**(3).

[17]. Congedo, P. M., Collura, S., & Congedo, P. M., (2009). Modeling and analysis of natural convection heat transfer in nanofluids, Proc. *ASME Summer Heat Transfer Conf.*, **3**:567-579.

[18]. Ghasemi, B., & Aminossadati, S. M., (2009). Natural convection heat transfer in an inclined enclosure filled with a water-Cuonanofluid, Numer. Heat Transfer; Part A: Applications **55**: 807-823.

[19]. Ho, C. J., Chen, M. W., & Li. Z. W., (2008). Numerical simulation of natural convection of nanofluid in a square enclosure: effects due to uncertainties of

viscosity and thermal conductivity. *Int. J. Heat Mass Transfer* **51**: 4506-4516.
[20]. Ho, C. J., Chen, M. W., & Li, Z. W., (2007). Effect of natural convection heat transfer of nanofluid in an enclosure due to uncertainties of viscosity and thermal conductivity, Proc. ASME/JSME *Thermal Engg. Summer Heat Transfer Conf*. HT, **1**: 833-841.
[21]. Das, S. K., Choi, S. U. S., Yu, W., & Pradeep, T., (2007). Nanofluids: *Science and Technology, Wiley, New Jersey.*